Radiology

Diffusion-weighted Imaging as a Treatment Response Biomarker for Evaluating Bone Metastases in Prostate Cancer: A Pilot Study[1]

Raquel Perez-Lopez, MD, MSc
Joaquin Mateo, MD, MSc
Helen Mossop, MMathStat
Matthew D. Blackledge, PhD
David J. Collins, BMIP
Mihaela Rata, PhD
Veronica A. Morgan, MS
Alison Macdonald, MS
Shahneen Sandhu, MD
David Lorente, MD
Pasquale Rescigno, MD
Zafeiris Zafeiriou, MD
Diletta Bianchini, MD
Nuria Porta, PhD
Emma Hall, PhD
Martin O. Leach, PhD
Johann S. de Bono, MB, ChB, PhD
Dow-Mu Koh, MD, FRCR, MRCP
Nina Tunariu, MD, FRCR, MRCP

Purpose: To determine the usefulness of whole-body diffusion-weighted imaging (DWI) to assess the response of bone metastases to treatment in patients with metastatic castration-resistant prostate cancer (mCRPC).

Materials and Methods: A phase II prospective clinical trial of the poly-(adenosine diphosphate–ribose) polymerase inhibitor olaparib in mCRPC included a prospective magnetic resonance (MR) imaging substudy; the study was approved by the institutional research board, and written informed consent was obtained. Whole-body DWI was performed at baseline and after 12 weeks of olaparib administration by using 1.5-T MR imaging. Areas of abnormal signal intensity on DWI images in keeping with bone metastases were delineated to derive total diffusion volume (tDV); five target lesions were also evaluated. Associations of changes in volume of bone metastases and median apparent diffusion coefficient (ADC) with response to treatment were assessed by using the Mann-Whitney test and logistic regression; correlation with prostate-specific antigen level and circulating tumor cell count were assessed by using Spearman correlation (r).

Results: Twenty-one patients were included. All six responders to olaparib showed a decrease in tDV, while no decrease was observed in all nonresponders; this difference between responders and nonresponders was significant ($P = .001$). Increases in median ADC were associated with increased odds of response (odds ratio, 1.08; 95% confidence interval [CI]: 1.00, 1.15; $P = .04$). A positive association was detected between changes in tDV and best percentage change in prostate-specific antigen level and circulating tumor cell count ($r = 0.63$ [95% CI: 0.27, 0.83] and $r = 0.77$ [95% CI: 0.51, 0.90], respectively). When assessing five target lesions, decreases in volume were associated with response (odds ratio for volume increase, 0.89; 95% CI: 0.80, 0.99; $P = .037$).

Conclusion: This pilot study showed that decreases in volume and increases in median ADC of bone metastases assessed with whole-body DWI can potentially be used as indicators of response to olaparib in mCRPC.

Published under a CC BY 4.0 license.

Online supplemental material is available for this article.

Prostate cancer is the second most commonly diagnosed cancer among men worldwide (1). Bone metastases are highly prevalent in patients with metastatic castration-resistant prostate cancer (mCRPC), the late stage of prostate cancer that causes substantial disease-related morbidity and mortality in this population. Bone metastases occur in up to 84% of patients with mCRPC and frequently represent the only site of metastatic disease (2).

Standard imaging techniques, such as computed tomography (CT) and technetium 99m bone scintigraphy, fail to allow accurate evaluation of the burden of bone metastases and detection of changes in response to treatment (3). In fact, the widely used Response Evaluation Criteria In Solid Tumors (RECIST) version 1.1 (4) do not define response in bone metastases, as this is considered to be nonmeasurable disease. The Prostate Cancer Working Group 2 criteria define progression in bone metastases on the basis of the appearance of new lesions at bone scintigraphy but fail to state any criteria for response in bone metastases (5). Therefore, evaluation of tumor response in patients with bone-only metastatic disease relies solely on decrease in prostate-specific antigen (PSA) level, which has not been proven to be a surrogate for improved survival (5–7). There is an urgent unmet need to identify, develop, and validate noninvasive response biomarkers for bone metastases in prostate cancer.

Diffusion-weighted imaging (DWI) is a functional magnetic resonance (MR) imaging technique used to study the motion of water molecules within tissue. Apparent diffusion coefficient (ADC) is an objective measurement of this water diffusion, which has been demonstrated to inversely correlate with cellularity in different tumor types, including bone marrow malignancies (8–13). Changes in ADC values after treatment have been correlated with tumor responses in different tumor types, including myeloma, ovarian carcinoma, primary peritoneal carcinoma, and rhabdomyosarcoma (14–16). Additionally, the volume of bone metastases assessed with whole-body DWI has prognostic value in patients with mCRPC (17). Limited data about the value of DWI in the assessment of response to bone metastases in mCRPC are currently available and come from small series of patients (18–21). In the setting of a prospective clinical trial, we aimed to determine the usefulness of whole-body DWI for the assessment of response of bone metastases to treatment in patients with mCRPC.

Materials and Methods

We conducted a phase II trial of the poly-(adenosine diphosphate–ribose) polymerase inhibitor olaparib (Lynparza; AstraZeneca, Cambridge, United Kingdom) in mCRPC (Trial of Olaparib in Patients with Advanced Castration-Resistant Prostate Cancer [TOPARP-A], Cancer Research UK no. CRUK/11/029); patients were enrolled from July 2012 to September 2014. A prospective MR imaging substudy was conducted with institutional review board approval at The Royal Marsden NHS Foundation Trust. Enrollment in this MR imaging substudy was optional; written informed consent was obtained for MR imaging acquisition.

Study Design

The primary end point of the TOPARP-A trial was response rate, with response defined as any of the following: a response of soft tissue and/or visceral

Advances in Knowledge

- All six patients who responded to the poly-(adenosine diphosphate–ribose) polymerase inhibitor olaparib showed a decrease in total diffusion volume (tDV) (median, −41.1%; range, −58.8% to −6.3%), but no decrease was observed in any of the 15 nonresponders (median, +20.7%; range, +0.0% to +76.9%); this difference between responders and nonresponders was significant (P = .001).

- Increases in median apparent diffusion coefficient of the tDV after 12 weeks of treatment were associated with responses to olaparib (odds ratio, 1.08; 95% confidence interval [CI]: 1.00, 1.15; P = .037).

- When analyzing up to five target bone metastases, changes in entire volume of the target bone metastases were also inversely associated with response (odds ratio, 0.89; 95% CI: 0.80, 0.99; P = .037).

Implication for Patient Care

- Clinical qualification of whole-body diffusion-weighted imaging as a response biomarker in bone metastases would improve assessment of response to treatment in metastatic castration-resistant prostate cancer, allowing for optimization of patient care, treatment decision making, and drug development in this common disease.

disease according to RECIST version 1.1 (4); a confirmed reduction of at least 50% in PSA level; or a conversion in the circulating tumor cell (CTC) count, with a reduction in the number of CTCs from at least five per 7.5 mL of blood at baseline to less than five per 7.5 mL of blood during treatment, with a confirmatory assessment at least 4 weeks later (22). Detailed information regarding the inclusion and exclusion criteria and the results of the TOPARP-A trial have been published and show a response rate of 33% (95% confidence interval [CI]: 20%, 48%) to olaparib in mCRPC (23).

Participation in the optional MR imaging substudy was offered to patients without contraindication to MR imaging at The Royal Marsden NHS Foundation Trust. Whole-body MR imaging was performed at baseline (within 28 days prior to starting treatment) and at cycle 4 day 1 (corresponding to 12 weeks after starting treatment) and every 12 weeks subsequently. The primary end point of the MR imaging substudy was to assess the association between changes in parameters derived from whole-body DWI (volume of bone metastases and median ADC) and response to olaparib. For MR imaging substudy purposes, patients were classified as responders if they met the definition of the primary end point of the TOPARP-A trial and if they had not experienced radiologic progression by 12 weeks.

Patient Population in the MR Imaging Substudy

Patients were included in this study if *(a)* signed informed consent was obtained for the MR imaging substudy in the setting of the TOPARP-A trial; *(b)* bone metastases were identified on images obtained with the combined imaging modalities of MR imaging, CT, and bone scintigraphy (in all cases); and *(c)* a minimum of two paired whole-body MR imaging studies were performed at baseline and after 12 weeks of treatment. Patients with whole-body MR images of suboptimal quality or incomplete studies were considered unevaluable for analysis and were excluded from the study.

Clinical Data Collection

Data were collated into an anonymized database and analyzed by the Institute of Cancer Research Clinical Trials and Statistical Unit, London, United Kingdom. PSA level and CTC counts were collected at baseline and every 12 weeks during treatment. CTC counts were also recorded at weeks 1, 2, 4, and 8. RECIST assessments were evaluated at baseline and every 12 weeks by using CT.

Whole-Body MR Imaging Parameters

Whole-body MR imaging was performed with a 1.5-T MR imaging unit (Avanto; Siemens Healthcare, Erlangen, Germany) by using surface and body coils in patients positioned supine. Axial images were acquired by using free-breathing single-shot twice-refocused echo-planar DWI from the upper cervical spine to the midthighs, sequentially across four imaging stations, each consisting of 50 sections. In addition to whole-body DWI, anatomic imaging was also performed by using breath-hold axial T1-weighted sequences. The imaging parameters are summarized in Table E1 (online).

Image Analysis

Images were processed and analyzed with open-access imaging assistant software (OsiriX version 5.6; PixmeoSARL, Bernex, Switzerland). Evaluation of T1-weighted and DWI images (ADC maps with b values of 50 and 900 sec/mm^2) was performed to assess the presence of metastatic bone disease. Regions of interest (ROIs) were delineated and included areas of abnormal signal intensity on DWI images obtained with b values of 900 sec/mm^2, which corresponded to high signal intensity on DWI images obtained with b values of 900 sec/mm^2 and low signal intensity on T1-weighted images, in keeping with metastatic bone disease. Different delineation techniques were undertaken for the abnormal signal intensity on DWI images obtained with b values of 900 sec/mm^2 that corresponded to bone metastases. First, ROI analyses were performed and included all areas of abnormal signal intensity on DWI images obtained with b values of 900 sec/mm^2 and T1-weighted MR images

that corresponded to bone metastases observed in the axial skeleton (spine and pelvis, not including the ribs) between C4 and the midthighs, labeled as total diffusion volume (tDV). Second, a more limited analysis was performed by using a RECIST approach with a maximum of five target representative bone metastases chosen by using the following criteria: maximum axial dimension larger than 1 cm, well-defined lesion border, and different skeletal areas represented. For this analysis, ROIs that included total volume of up to five target lesions and ROIs that included the central section of the same target lesions were chosen.

Additionally, one radiologist (R.P.L.) manually delineated the entire axial skeleton (spine and pelvis, not including the ribs) by including normal and abnormal bone marrow from C4 to the lesser trochanters. This delineation technique was included in view of its possible advantage for automated segmentation of the skeleton.

A semiautomated segmentation tool from OsiriX version 5.6 (PixmeoSARL) was used for delineating ROIs. All the delineation techniques for whole-body DWI images were performed by one radiologist (R.P.L.) with 3 years of experience in whole-body DWI; manual correction of the segmentation mask that corresponded to the ROIs was performed by the radiologist where necessary (Fig 1). The volume of metastases was calculated as the number of voxels for all ROIs, multiplied by the voxel volume in each case. The ADC value for every pixel was recorded, and histogram representations of the ADC values of bone metastases for each patient were generated by using Microsoft Excel 2010 (Microsoft, Redmond, Wash).

Statistical Analysis

Distribution of PSA level, CTC counts, median ADC values, tDV, volume, and diameter of the target lesions at baseline and percentage change after 12 weeks of treatment were presented by using descriptive statistics. Baseline distributions and median changes during treatment in ADC, tDV, volume, and diameter of the target lesions were compared between
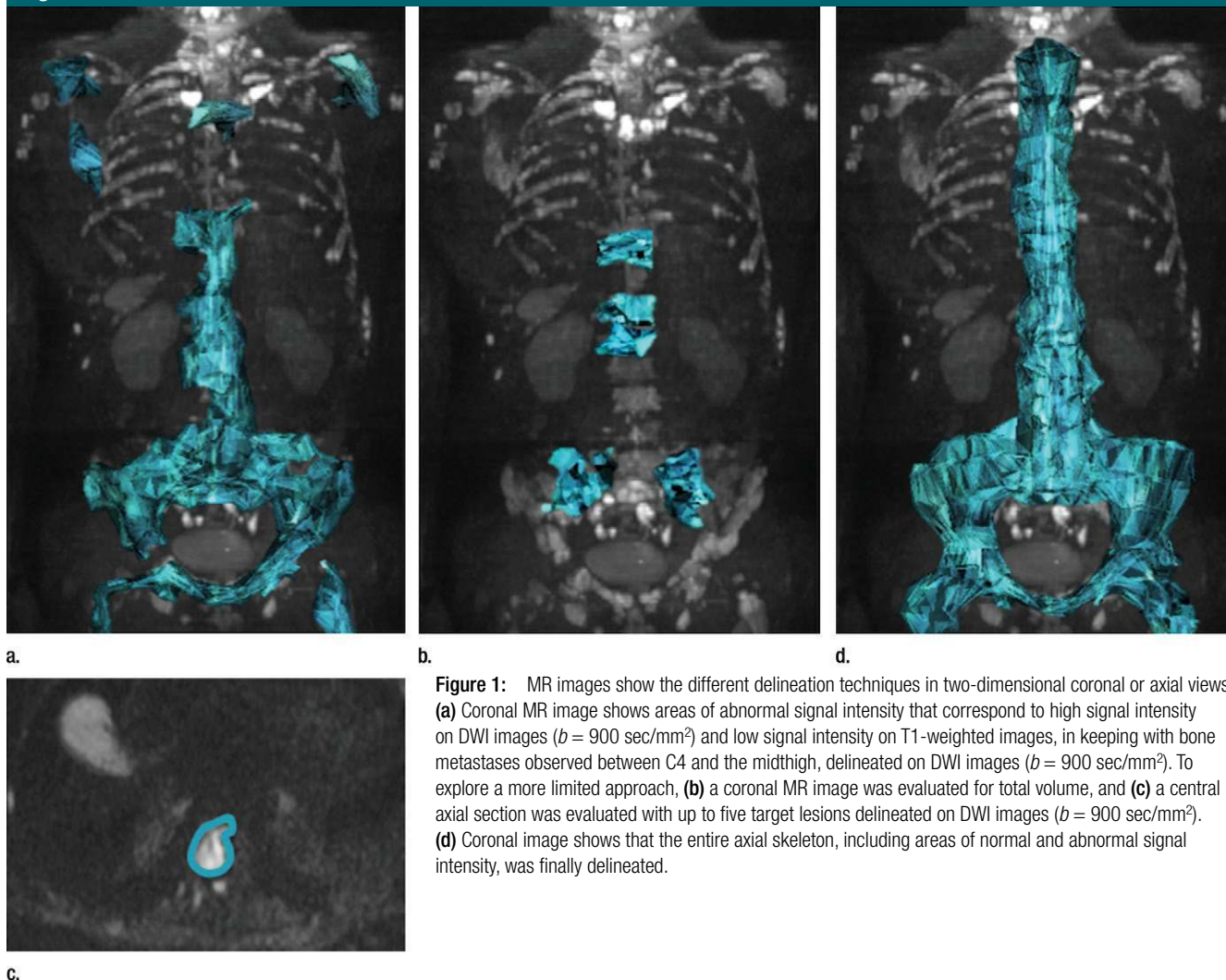
Figure 1

Figure 1:   MR images show the different delineation techniques in two-dimensional coronal or axial views. **(a)** Coronal MR image shows areas of abnormal signal intensity that correspond to high signal intensity on DWI images ($b = 900$ sec/mm^2) and low signal intensity on T1-weighted images, in keeping with bone metastases observed between C4 and the midthigh, delineated on DWI images ($b = 900$ sec/mm^2). To explore a more limited approach, **(b)** a coronal MR image was evaluated for total volume, and **(c)** a central axial section was evaluated with up to five target lesions delineated on DWI images ($b = 900$ sec/mm^2). **(d)** Coronal image shows that the entire axial skeleton, including areas of normal and abnormal signal intensity, was finally delineated.

responders and nonresponders by using nonparametric Mann-Whitney tests, and their association with response to treatment was compared by using univariate and multivariate logistic regression models (adjusted for known prognostic factors of baseline PSA level, lactate dehydrogenase level, and alkaline phosphatase level). The correlation between *(a)* baseline tDV and changes in tDV after 12 weeks of treatment and *(b)* baseline and best percentage change in PSA level and CTC count, respectively, were assessed by using the Spearman correlation coefficient *(r)*, with *r* values of at least 0.4 and less than 0.6 indicating moderate correlation, at least 0.6

and less than 0.8 indicating strong correlation, and at least 0.8 indicating very strong correlation. A significance level of .05 and 95% confidence intervals (CIs) have been used. No adjustment for reporting of multiple analyses was performed; therefore, significant results must be interpreted with caution. The analyses are based on a data snapshot obtained on April 24, 2015, and were performed with Stata version 13 software (StataCorp, College Station, Tex).

Results

Thirty-two of the 42 patients (76.2%) enrolled in the TOPARP-A trial at The

Royal Marsden NHS Foundation Trust consented to the MR imaging substudy. Six patients did not undergo baseline whole-body MR imaging because of logistical or technical issues. All 26 patients with whole-body MR images at baseline had bone metastases. Of the 26 patients with baseline whole-body MR images, five did not undergo whole-body MR imaging at 12 weeks because of poor performance status. None of the cases were excluded for having suboptimal quality of the whole-body MR images or incomplete studies. Therefore, 21 patients had evaluable whole-body MR images at baseline and after 12 weeks of treatment (Fig 2); the

median age of all patients was 68.2 years (range, 40.8–79.3 years). The population characteristics at baseline are summarized in Table 1. The baseline CT images were also reviewed by using previously described terminology (24); 19 of the 21 patients had sclerotic bone metastases, whereas two patients had mixed osteoblastic and osteolytic disease with predominantly lytic metastases. The other sites of metastatic disease observed outside the bone were in lymph nodes (57.1%, 12 of 21 patients), liver (28.6%, six of 21 patients), and lung (23.8%, five of 21 patients). Seven patients had bone metastases only at baseline (33.3%, seven of 21). Six patients (28.6%, six of 21) were considered responders to olaparib per the primary end point definition and had not progressed prior to 12 weeks.

The median time between baseline whole-body MR imaging and the start of treatment was 6 days (1st quartile, 2.5 days; 3rd quartile, 11 days). The absolute value of the tDV, the sum of the five target lesion total volumes and of the central section diameters, and the median ADC at baseline assessed by using the different delineation techniques are summarized according to response status in Table 2. The percentage change of these parameters after 12 weeks of treatment is summarized according to response status in Table 3 and represented in box plots in Figure E1 (online).

Analysis of Axial Skeleton DWI with a *b* Value of 900 sec/mm² and Abnormal Signal Intensity

When delineating all the areas of abnormal DWI signal intensity, in keeping with bone metastases in the axial skeleton, the median tDV in this population was 0.45 L (range, 0.01–1.31 L), and median ADC was 782×10^{-6} mm²/sec (range, $[684–1121] \times 10^{-6}$ mm²/sec). These parameters, grouped according to responders and nonresponders, are summarized in Table 2; there were no statistically significant differences between baseline distribution of tDV and median ADC between the two groups ($P = .243$ and $P = .312$, respectively).
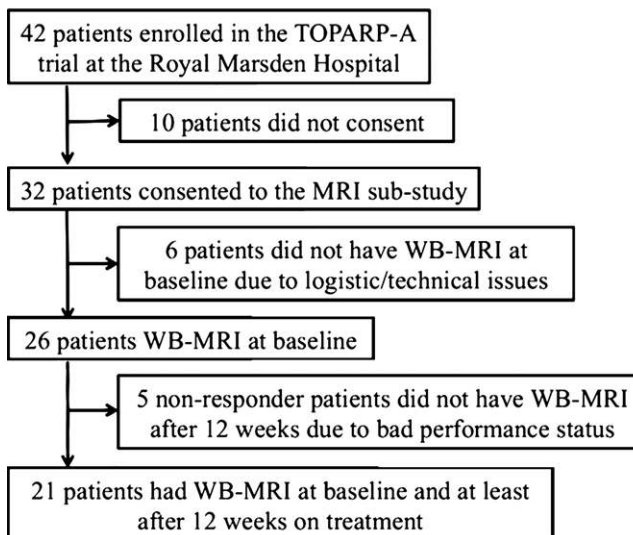
Figure 2

Figure 2: Consort diagram shows the study selection process. *WB* = whole-body.

Table 1

Baseline Characteristics and Prior Treatments in All 21 Patients

Parameter	Value
Clinical characteristic	
Hemoglobin level (g/dL)*	10.9 (10.2, 11.5) [9.2–14.2]
PSA level (ng/mL)*	411 (146, 806) [19–2949]
Alkaline phosphatase level (IU/L)*	147 (86, 363) [54–2652]
Lactate dehydrogenase level (IU/L)*	234 (176, 318) [109–862]
Albumin level (g/dL)*	3.5 (3.1, 3.7) [2.7–4.0]
CTC count (no. per 7.5 mL)*	46 (8, 102) [3–187]
Prior treatment	
Docetaxel	21 (100)
Cabazitaxel	11 (52.4)
Abiraterone acetate	19 (90.5)
Enzalutamide	4 (19.0)
Radium 223	1 (4.8)
Bisphosphonates	4 (19.0)
Palliative radiation therapy to bone	6 (28.6)
Site of metastatic disease	
Bone	21 (100)
Nodes	12 (57.1)
Liver	6 (28.6)
Lung	5 (23.8)
Bone only	7 (33.3)

Note.—Unless indicated otherwise, data are numbers of patients, with percentages in parentheses. To convert grams per deciliter to grams per liter, multiply by 10. To convert nanograms per milliliter to micrograms per liter, multiply by 1.0. To convert international units per liter to microkatals per liter, multiply by 0.0167.

* Data are medians, with 1st and 3rd quartiles in parentheses and ranges in brackets.

Table 2

Baseline Parameters of Bone Metastases Assessed in Responders and Nonresponders

Parameter	Responders		Nonresponders		P Value*
	No. of Patients	Median	No. of Patients	Median	
Clinical characteristic					
CTC count (no. per 7.5 mL)	6	63 (8, 102) [3–105]	15	46 (8, 104) [6–187]	.845
PSA level (ng/mL)	6	868 (34, 1847) [28–2949]	15	381 (146, 456) [19–1505]	.350
Axial skeleton, abnormal DWI signal intensity					
Volume (L)	6	0.83 (0.17, 1.01) [0.16–1.31]	15	0.44 (0.16, 0.79) [0.01–1.07]	.243
ADC ($\times 10^{-6}$ mm²/sec)	6	847 (775, 921) [693–1121]	15	748 (726, 915) [684–1023]	.312
Up to five target lesions					
Volume (L)	6	0.05 (0.04, 0.06) [0.04–0.09]	15	0.05 (0.02, 0.12) [0.01–0.52]	.876
ADC ($\times 10^{-6}$ mm²/sec)	6	859 (814, 900) [606–1712]	15	737 (695, 865) [624–1017]	.312
Central section, five target lesions					
Diameter (mm)	2	15.3 (14.3, 16.3) [14.3–16.3]	7	11.6 (7.5, 13.1) [2.8–20.2]	.143
Median ADC ($\times 10^{-6}$ mm²/sec)	6	941 (867, 1002) [555–1263]	15	743 (673, 852) [575–1083]	.073
Entire axial skeleton					
ADC ($\times 10^{-6}$ mm²/sec)	6	808 (650, 1093) [614–1182]	15	805 (751, 1002) [722–1039]	.938

Note.—Numbers in parentheses are 1st and 3rd quartiles. Numbers in brackets are ranges. To convert nanograms per milliliter to micrograms per liter, multiply by 1.0.

* According to the Mann-Whitney test.

Table 3

Percentage Change after 12 Weeks of Treatment in Responders and Nonresponders

Parameter	Responders		Nonresponders		P Value*
	No. of Patients	Median Change (%)	No. of Patients	Median Change (%)	
Clinical characteristic					
CTC count	6	−96.0 (−100, −82.9) [−100 to −60.5]	15	−2.9 (−37.5, 75.0) [−73.8 to 312.5]	NA†
PSA level	6	−68.6 (−80.1, −37.5) [−94.6 to −29.3]	15	89.9 (36.0, 239.0) [−14.4 to 525.6]	NA†
Axial skeleton, abnormal DWI signal intensity					
Volume	6	−41.1 (−52.9, −28.7) [−58.8 to −6.3]	15	20.7 (3.2, 53.0) [0.0–76.9]	.001
ADC	6	35.4 (3.8, 44.1) [1.3–59.5]	15	7.5 (3.7, 15.6) [−9.0 to 32.7]	.139
Up to five target lesions					
Volume	6	−25.5 (−57.0, −18.2) [−78.7 to 4.54]	15	14.6 (0.0, 47.5) [−20.2 to 76.9]	.002
ADC	6	26.3 (11.4, 47.4) [4.8–102.9]	15	7.4 (−2.3, 12.9) [−10.8 to 25.6]	.024
Central section, five target lesions					
Diameter	2	−59.2 (−88.3, −30.1) [−88.3 to −30.1]	7	3.8 (1.6, 41.4) [0.0–69.9]	.040
ADC	6	27.4 (14.0, 47.0) [12.8–52.3]	15	10.0 (3.2, 17.2) [−12.7 to 63.1]	.018
Entire axial skeleton					
ADC	6	7.4 (−0.8, 26.0) [−16.6 to 29.0]	15	5.6 (3.4, 12.5) [−21.6 to 16.7]	.876

Note.—Numbers in parentheses are 1st and 3rd quartiles. NA = not applicable. Numbers in brackets are ranges.

* Changes in CTC count and PSA level were used to define response and nonresponse; therefore, formal comparisons have not been made.

† According to the Mann-Whitney test.

All six patients who responded to olaparib showed a decrease in tDV (median, −41.1%; range, −58.8% to −6.3%), but no decrease was observed in any of the 15 nonresponders (median, +20.7%; range, +0.0% to +76.9%); this difference between responders and nonresponders was significant (P = .001) (Table 3, Fig E1 [online]). Patients who responded to olaparib showed a greater increase in median ADC after 12 weeks of treatment (median: +35.4%; range, +1.3% to +59.5%), compared with nonresponders (median, +7.5%; range,

−9.0% to +32.7%; P = .14); increases in median ADC after 12 weeks of treatment were associated with increased odds of response (odds ratio, 1.08; 95% CI: 1.00, 1.15; P = .037) (Table 4, Fig E2 [online]). An example of a responding patient is represented in Figure 3.

The two patients with mixed osteoblastic and osteolytic pattern with predominantly lytic bone metastases were nonresponders who had +55.5% and +24.6% increase in tDV and +3.40% and + 15.6% increase in median ADC, respectively, after 12 weeks of treatment.

The correlation between PSA levels, CTC counts, and DWI parameters was also explored; baseline PSA levels and CTC counts showed strong and moderate positive association with baseline tDV (r = 0.64 [95% CI: 0.29, 0.84] and r = 0.59 [95% CI: 0.22–0.82], respectively), and there was a strong positive association between changes in tDV and best posttreatment percentage change in PSA level and CTC count (r = 0.63 [95% CI: 0.27, 0.83] and r = 0.77 [95% CI: 0.51, 0.90], respectively), indicating that changes in tDV correlate with response to therapy.

Of the six responding patients, four underwent further evaluable whole-body MR imaging at the time of radiologic progression and/or with PSA level increase. In all four patients, we observed a decrease in tDV while responding to olaparib, followed by a later increase in tDV at the time of radiologic progression and/or increase in PSA level. Three of these four responding patients also had an increase in median ADC while responding to treatment, followed by a decrease in median ADC at the time of radiologic progression and/or increase in PSA level. The fourth patient experienced minimal median ADC change at the PSA level nadir and at disease progression (Figs E3, E4 [online]).

Analysis of Five Target Lesions (Total Volume and Central Section)

With the aim of evaluating more limited radiologic analyses, to decrease workload, we correlated changes in up to five target lesions per patient with treatment response. We evaluated five target lesions in 19 of the 21 patients (90.5%); the remaining two patients had only one and three evaluable bone lesions, respectively. The median sum of total volumes that corresponded to the target lesions in the population at baseline was 0.05 L (range, 0.01–0.52 L), and the median ADC when delineating total volume of the target lesions was 814 × 10^{-6} mm^2/sec (range, [606–1712] × 10^{-6} mm^2/sec). In patients with nonwidespread bone disease (n = 9), we also assessed the diameter of the target lesions in the central section. When assessing only the central section of the same target lesions, the median of the sum of diameters at baseline was 12.6 mm (range, 2.8–20.2 mm), and the median ADC was 835 × 10^{-6} mm^2/sec (range, [554.5–1263] × 10^{-6} mm/sec). These parameters, grouped according to responders and nonresponders, are summarized in Table 2; there were no statistically significant differences between the baseline distribution of volume, diameter, and median ADC (central section and volume) of the target lesions between the two groups (P = .876, P = .143, P = .312, and P = .073, respectively).

Then, we assessed the same target lesions for each patient on their follow-up whole-body MR images after 12 weeks of treatment; the percentage change of these parameters after 12 weeks of treatment is summarized according to response status in Table 3 and Figure E1 (online). Changes in entire lesion volume of the target bone metastases were also inversely associated with response (odds ratio, 0.89; 95% CI: 0.80, 0.99; P = .037) (Table 4). The median ADC change at 12 weeks, when analyzing the target bone metastases (total volume and central section), was also associated with response, although these associations did not reach statistical significance (P = .056 and P = .082, respectively) (Table 4). Results from the multivariate logistic regression analyses showed similar trends (Table 4).

Analysis of the Axial Skeleton (Including Normal and Abnormal Bone Marrow)

The baseline median ADC in our population when delineating the entire axial skeleton, including both normal and abnormal bone marrow, was 805 × 10^{-6} mm^2/sec (range, [614–1182] × 10^{-6} mm^2/sec). Median ADC values at baseline, grouped according to

Table 4

Logistic Regression Associations between Changes in Values after 12 Weeks with Binary Response to Treatment

Parameter	No. of Patients	Univariate Analysis		Multivariate Analysis*	
		Odds Ratio	P Value	Odds Ratio	P Value
Axial skeleton DWI signal intensity abnormality					
Volume	21	Not calculable[†]	…	Not calculable[†]	…
Median ADC	21	1.08 (1.00, 1.15)	.037	1.16 (1.01, 1.33)	.04
Up to five target lesions					
Volume	21	0.89 (0.80, 0.99)	.037	0.53 (0.09, 3.15)	.48
Median ADC	21	1.10 (1.00, 1.22)	.056	1.13 (0.95, 1.33)	.17
Central section five target lesions					
Median ADC	21	1.05 (0.99, 1.11)	.082	1.07 (0.99, 1.15)	.07
Entire axial skeleton					
Median ADC	21	1.03 (0.94, 1.12)	.518	1.03 (0.93, 1.15)	.56

Note.—Numbers in parentheses are 95% CIs.

* Adjusted for baseline PSA level, lactate dehydrogenase level, and alkaline phosphatase level.

[†] Unable to fit model, as change in volume < 0% predicts data perfectly.
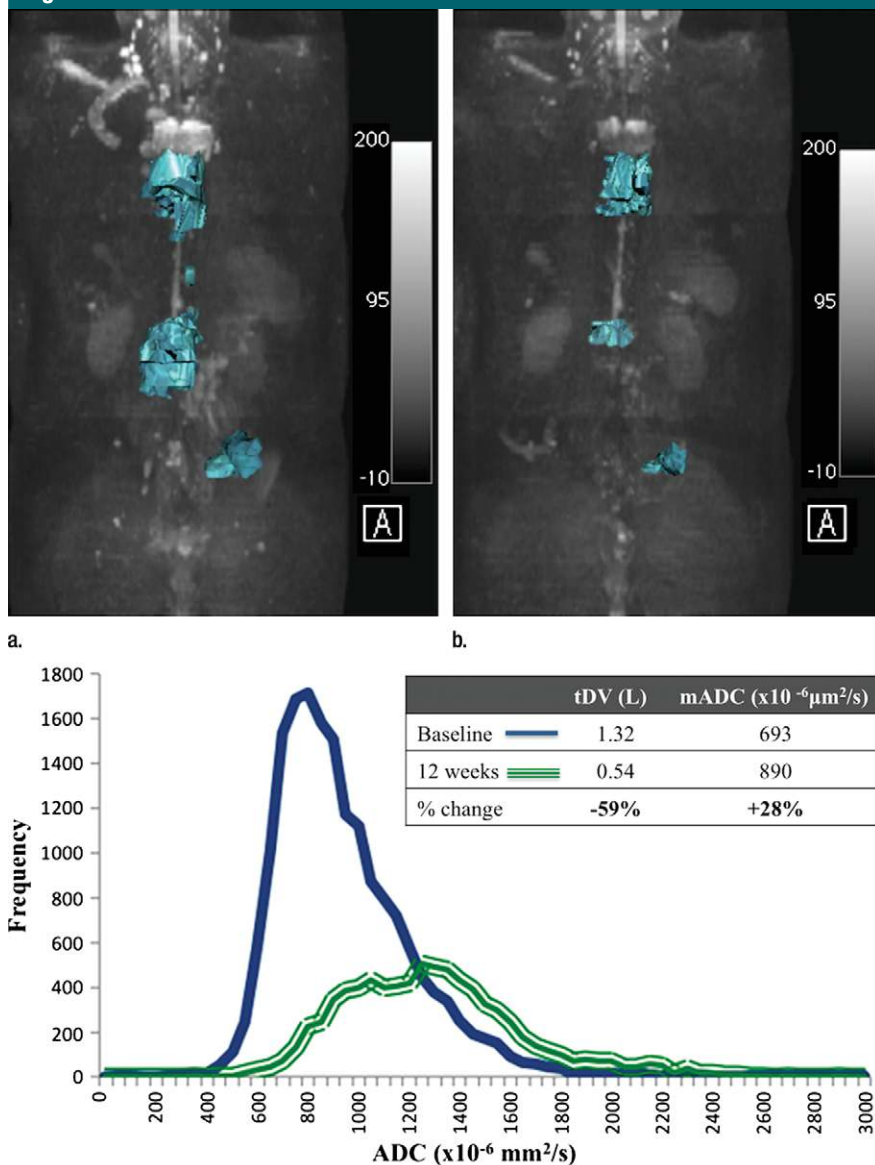
Figure 3

Figure 3: **(a)** Coronal baseline MR image and **(b)** coronal MR image obtained after 12 weeks of treatment in a 70-year-old man with mCRPC responding to olaparib show a reduction in the abnormal DWI signal intensity ($b = 900$ sec/mm^2) extent on maximum intensity projection images. **(c)** Histogram depicts the ADC values of the tDV at baseline and after 12 weeks of treatment, showing an increase in the median ADC.

responders and nonresponders, are summarized in Table 2; there were no statistically significant differences between the baseline distributions of median ADC between the two groups ($P = .94$). The percentage change in median ADC after 12 weeks of treatment is summarized according to response status in Table 3 and Figure E1 (online). When comparing the median ADC of the entire axial skeleton (normal and abnormal bone marrow) before and after treatment with olaparib, changes in median ADC were not associated with response to treatment ($P = .518$) (Table 4).

Discussion

We hypothesized that changes in volume of bone marrow metastases assessed with DWI and changes in median ADC are indicators of response of bone metastases to treatment in patients with mCRPC. In our study, we explored different delineation techniques for assessing bone metastases quantitatively and qualitatively with whole-body DWI. One technique included all the areas of DWI signal abnormality, in keeping with all bone metastases in the axial skeleton (tDV); the other focused on two simpler techniques for assessing five target lesions, based on the widely used RECIST version 1.1 (4), to determine whether a simplified approach may be viable in clinical practice. Finally, we explored whether changes in median ADC that delineate the entire spine and pelvis (including areas of normal and abnormal bone marrow), which may facilitate automated delineation, were associated with response.

We have shown that when delineating all the areas of DWI signal intensity abnormality, in keeping with bone metastases in the axial skeleton (from C4 to midthigh), the changes detected in tDV and median ADC after 12 weeks of treatment allow the identification of responders in mCRPC with bone metastases. Decreases in tDV correlated with decreases in PSA level and CTC count and with overall response, as defined as a composite end point in the TOPARP-A clinical trial (23). Consistent with the fact that tumor cell death results in increased water diffusivity, manifested as higher ADC values, patients who responded to olaparib also showed a greater increase in median ADC when compared with nonresponders. In our population, the results of simpler ways of assessing bone metastases on whole-body DWI images in five selected target lesions (total volume or central section) support further evaluation of this faster and more practical approach in future studies, as decreases in volume and diameter of the five target lesions after 12 weeks of treatment were associated with response. There was also a trend of significance when associating median

ADC increases of the target lesions at 12 weeks and response. Therefore, overall, these data indicate that whole-body DWI may have a role in bone metastases response assessment in mCRPC, without the need for ionizing radiation or intravenous contrast material, potentially allowing the detection of differential responses in visceral or nodal metastases and bone metastases. Clinical qualification of whole-body DWI as a response biomarker in bone metastases would improve assessment of response to treatment in mCRPC, allowing for optimization of patient care, treatment decision making, and drug development in this common disease. Conversely, when delineating the spine and pelvis, including all areas of normal and abnormal bone marrow, increases in median ADC after 12 weeks of treatment were not associated with response, probably because of the fact that changes in median ADC in bone metastases are diluted by the absence of changes in median ADC in normal bone marrow.

We acknowledge the potential limitations of our study. First, because of the small size of this pilot study, only limited exploration of the effect of adjustment for other clinical factors on the association of changes in tDV and median ADC is possible. Analyzing larger populations in multicenter studies is now needed for future validation of these results and to allow multivariate analyses. Second, all our patients were treated with one drug, the poly-(adenosine diphosphate–ribose) polymerase inhibitor olaparib; however, in previous studies, investigators identified similar changes in DWI in bone metastases responding to hormonal therapy and cytotoxic agents (18–21). Prospective studies conducted to replicate our results with established treatments for mCRPC are now needed. Third, it should be noted that ROI delineation depends on the quality of the acquired DWI data, the semiautomatic segmentation tool, and the radiologist's expertise. In prior studies, investigators reported high intrareader reproducibility of DWI analysis by using similar bone metastases delineation methods

(17,25), although this needs to be validated in larger, properly powered studies. Finally, we acknowledge that most of our population had sclerotic bone metastases; only two patients had predominantly lytic bone metastases, and therefore, it was not feasible to perform comparisons between the sclerotic and lytic nature of the bone metastases. Despite these limitations, our study represents the largest prospective series to date in a trial of a novel therapeutic assessment of response to drug treatment in bone metastases in patients with mCRPC by using whole-body DWI. The data presented here highlight the potential of DWI for bone metastases response assessment and warrants further evaluation of whole-body DWI in this disease.

In conclusion, we have shown that assessment of bone metastases with whole-body DWI during anticancer treatment is feasible, with changes in bone metastases volume and median ADC being indicators of response to treatment in mCRPC in our pilot study. Moreover, the more efficient study of five target lesions has substantial practical merit for disease evaluation, which can be more easily adopted into clinical practice. These results support further evaluation of DWI as a response biomarker in prospective mCRPC patient cohorts, ideally embedded into clinical trials (26).

References

1. Ferlay J, Soerjomataram I, Dikshit R, et al. Cancer incidence and mortality worldwide: sources, methods and major patterns in GLOBOCAN 2012. Int J Cancer 2015; 136(5):E359–E386.

2. Gandaglia G, Abdollah F, Schiffmann J, et al. Distribution of metastatic sites in patients with prostate cancer: a population-based analysis. Prostate 2014;74(2):210–216.

3. Jambor I, Kuisma A, Ramadan S, et al. Prospective evaluation of planar bone scintigraphy, SPECT, SPECT/CT, 18F-NaF PET/CT and whole body 1.5T MRI, including DWI, for the detection of bone metastases in high risk breast and prostate cancer patients: SKELETA clinical trial. Acta Oncol 2016;55(1):59–67.

4. Eisenhauer EA, Therasse P, Bogaerts J, et al. New response evaluation criteria in solid tumours: revised RECIST guideline (version 1.1). Eur J Cancer 2009;45(2):228–247.

5. Scher HI, Halabi S, Tannock I, et al. Design and end points of clinical trials for patients with progressive prostate cancer and castrate levels of testosterone: recommendations of the Prostate Cancer Clinical Trials Working Group. J Clin Oncol 2008;26(7): 1148–1159.

6. Berthold DR, Pond GR, Roessner M, et al. Treatment of hormone-refractory prostate cancer with docetaxel or mitoxantrone: relationships between prostate-specific antigen, pain, and quality of life response and survival in the TAX-327 study. Clin Cancer Res 2008;14(9):2763–2767.

7. Halabi S, Armstrong AJ, Sartor O, et al. Prostate-specific antigen changes as surrogate for overall survival in men with metastatic castration-resistant prostate cancer treated with second-line chemotherapy. J Clin Oncol 2013;31(31):3944–3950.

8. Guo AC, Cummings TJ, Dash RC, Provenzale JM. Lymphomas and high-grade astrocytomas: comparison of water diffusibility and histologic characteristics. Radiology 2002; 224(1):177–183.

9. Hayashida Y, Hirai T, Morishita S, et al. Diffusion-weighted imaging of metastatic brain tumors: comparison with histologic type and tumor cellularity. AJNR Am J Neuroradiol 2006;27(7):1419–1425.

10. Zelhof B, Pickles M, Liney G, et al. Correlation of diffusion-weighted magnetic resonance data with cellularity in prostate cancer. BJU Int 2009;103(7):883–888.

11. Liu Y, Ye Z, Sun H, Bai R. Clinical application of diffusion-weighted magnetic resonance imaging in uterine cervical cancer. Int J Gynecol Cancer 2015;25(6):1073–1078.

12. Matsubayashi RN, Fujii T, Yasumori K, Muranaka T, Momosaki S. Apparent diffusion coefficient in invasive ductal breast carcinoma: correlation with detailed histologic features and the enhancement ratio on dynamic contrast-enhanced MR images. J Oncol 2010;2010:2010.

13. Nonomura Y, Yasumoto M, Yoshimura R, et al. Relationship between bone marrow cellularity and apparent diffusion coefficient. J Magn Reson Imaging 2001;13(5):757–760.

14. Thoeny HC, De Keyzer F, Chen F, et al. Diffusion-weighted MR imaging in monitoring the effect of a vascular targeting agent on rhabdomyosarcoma in rats. Radiology 2005; 234(3):756–764.

15. Kyriazi S, Collins DJ, Messiou C, et al. Metastatic ovarian and primary peritoneal cancer: assessing chemotherapy response with diffusion-weighted MR imaging—value of histogram analysis of apparent diffusion coefficients. Radiology 2011;261(1):182–192.

16. Giles SL, Messiou C, Collins DJ, et al. Whole-body diffusion-weighted MR imaging for assessment of treatment response in myeloma. Radiology 2014;271(3):785–794.

17. Perez-Lopez R, Lorente D, Blackledge MD, et al. Volume of bone metastasis assessed with whole-body diffusion-weighted imaging is associated with overall survival in metastatic castration-resistant prostate cancer. Radiology 2016;280(1):151–160.

18. Blackledge MD, Collins DJ, Tunariu N, et al. Assessment of treatment response by total tumor volume and global apparent diffusion coefficient using diffusion-weighted MRI in patients with metastatic bone disease: a feasibility study. PLoS One 2014;9(4):e91779.

19. Reischauer C, Froehlich JM, Koh DM, et al. Bone metastases from prostate cancer: assessing treatment response by using diffusion-weighted imaging and functional diffusion maps—initial observations. Radiology 2010;257(2):523–531.

20. Lee KC, Bradley DA, Hussain M, et al. A feasibility study evaluating the functional diffusion map as a predictive imaging biomarker for detection of treatment response in a patient with metastatic prostate cancer to the bone. Neoplasia 2007;9(12):1003–1011.

21. Messiou C, Collins DJ, Giles S, de Bono JS, Bianchini D, de Souza NM. Assessing response in bone metastases in prostate cancer with diffusion weighted MRI. Eur Radiol 2011;21(10):2169–2177.

22. Olmos D, Arkenau HT, Ang JE, et al. Circulating tumour cell (CTC) counts as intermediate end points in castration-resistant prostate cancer (CRPC): a single-centre experience. Ann Oncol 2009;20(1):27–33.

23. Mateo J, Carreira S, Sandhu S, et al. DNA-repair defects and olaparib in metastatic prostate cancer. N Engl J Med 2015;373(18): 1697–1708.

24. Vargas HA, Wassberg C, Fox JJ, et al. Bone metastases in castration-resistant prostate cancer: associations between morphologic CT patterns, glycolytic activity, and androgen receptor expression on PET and overall survival. Radiology 2014;271(1): 220–229.

25. Blackledge MD, Tunariu N, Orton MR, et al. Inter- and intra-observer repeatability of quantitative whole-body, diffusion-weighted imaging (WBDWI) in metastatic bone disease. PLoS One 2016;11(4):e0153840.

26. Yap TA, Sandhu SK, Workman P, de Bono JS. Envisioning the future of early anticancer drug development. Nat Rev Cancer 2010;10(7):514–523.